Cerebroside Sulfotransferase Forms Homodimers in Living Cells†

Afshin Yaghootfam, Thomas Sorkalla, Hanns Häberlein, Volkmar Gieselmann, Joachim Kappler, and Matthias Eckhardt*

Institut für Physiologische Chemie, Rheinische Friedrich-Wilhelms-Universität Bonn, Germany

Received January 4, 2007; Revised Manuscript Received May 19, 2007

ABSTRACT: Cerebroside sulfotransferase (CST) catalyzes the 3′-sulfation of galactose residues in several glycolipids. Its major product in the mammalian brain is sulfatide, which is an essential myelin component. Using epitope-tagged variants, murine CST was found to localize to the Golgi apparatus, but in contrast to previous assumptions, not to the trans-Golgi network. An examination of enhanced green fluorescent protein (EGFP)-tagged CST suggests that CST forms homodimers and that dimerization is mediated by the lumenal domain of the enzyme, as shown by immunoprecipitation and density gradient centrifugation. In order to verify that dimerization of CST observed by biochemical methods reflects the behavior of the native protein within living cells, the mobility of CST-EGFP was examined using fluorescence correlation spectroscopy. These experiments confirmed the homodimerization of CST-EGFP fusion proteins in vivo. In contrast to full-length CST, a fusion protein of the amino-terminal 36 amino acids of CST fused to EGFP was exclusively found as a monomer but nevertheless showed Golgi localization.

Cerebroside sulfotransferase (CST[1]) is a type II membrane protein transferring sulfate to the 3′-OH group of galactose (*1*). CST has been purified, and its cDNA was cloned from humans and mice (*2*, *3*). Human and murine CSTs contain two putative N-glycosylation sites (at amino acid positions 66 and 312), which are both glycosylated. We described previously that N-glycosylation of Asn-312 and Asn-66 is required for the full expression of catalytic activity (*4*). Products of CST are lipids, the two most abundant are the glycosphingolipid 3-*O*-sulfogalactosylceramide (sulfatide), which is found in high concentrations in the brain and kidney (*5*, *6*), and the glycerolipid 3-*O*-sulfogalactosyl-1-alkyl-2-acyl-glycerol (seminolipid), a major glycolipid in the testis (*7*). Sulfatide and seminolipid fulfill important functions in various physiological processes, such as regulation of oligodendrocyte differentiation (*8*), formation of paranodes at the nodes of Ranvier (*9*), and spermatogenesis (*5*, *7*). As shown recently, deficiency in CST results in the complete absence of sulfatide and seminolipid in mice (*10*). In the absence of sulfatide, oligodendrocyte precursor cells exhibited a significant acceleration of their differentiation into mature oligodendrocytes *in vitro* and *in vivo* (*8*), suggesting that sulfatide is an inhibitor of oligodendrocyte differentiation. Sulfatide accumulation, however, causes metachromatic leukodystrophy (MLD), a lysosomal storage disorder that results from a deficiency in arylsulfatase A (ASA) (*11*). A causative therapy is not available, and patients die after years of illness. Recent progress in the therapy of lysosomal storage disorders provided strong evidence for the feasibility of substrate reduction therapy in lysosomal storage disorders (*12*, *13*). Thus, inhibition of CST could also be an option for the treatment of MLD.

Several glycosyltransferases of the Golgi apparatus form homo or heterodimers, and some also form larger oligomers (*14*, *15*). Golgi localization of some glycosyltransferases correlates with their ability to oligomerize according to the kin recognition model of Golgi retention (*16*). Here, we show that CST resides in the Golgi apparatus and not in the trans-Golgi network (TGN), in contrast to previous assumptions (*17*). The transmembrane domain of CST, together with flanking lysine residues, was sufficient to localize a green fluorescence reporter protein to the Golgi apparatus. Moreover, we could show in this study that CST forms homodimers in living cells.

MATERIALS AND METHODS

Antibodies. Antibodies against HA-tag (clone 12CA5) was purchased from Roche (Mannheim, Germany), and rabbit anti-EGFP antibody was from Abcam. Mouse monoclonal anti-EGFP antibody was from Chemicon. Antisera against α-mannosidase II (αManII) and 300 kDa mannose 6-phosphate receptor (MPR300) were kindly provided by K. Moremen (University of Georgia) and P. Saftig (University of Kiel, Germany), respectively. Mouse antibody against polysialic acid NCAM (PSA-NCAM) was kindly provided by R. Gerardy-Schahn (Medical school, Hannover). Cy2- and Cy3-conjugated goat anti-rabbit immunglobulines were from Jackson Immuno Research Laboratories (West Grove, PA). Dulbecco's modified Eagle's medium (DMEM), DMEM/

† This work was supported by the Deutsche Forschungsgemeinschaft through SFB 645 of the University of Bonn.

* To whom correspondence should be addressed. Dr. Matthias Eckhardt, Institut für Physiologische Chemie, Rheinische Friedrich-Wilhelms-Universität Bonn, Nussallee 11, D-53115 Bonn, Germany. Tel: +49-228-73-4735. Fax: +49-228-73-2416. E-mail: eckhardt@institut.physiochem.uni-bonn.de.

[1] Abbreviations: αManII, α-mannosidase II; ASA, arylsulfatase A; BHK, baby hamster kidney; BFA, brefeldin A; CHO, chinese hamster ovary; CST, cerebroside sulfotransferase; DAPI, 4′,6-diamidino-2-phenylindole; EGFP, enhanced green fluorescent protein; ER, endoplasmic reticulum; HA, hemaglutinin; MLD, metachromatic leukodystrophy; MPR300, 300 kDa mannose 6-phosphate receptor; TGN, trans-Golgi network.

10.1021/bi700014q CCC: $37.00
Published on Web 07/21/2007

Table 1: Oligonucleotides Used to Generate EGFP Fusion Proteins with CST Mutants[a]

construct	primers	PCR template
pCST-EGFP	GCCTCGAGCCATGACTCTGCTGCCAAAGAAGCC GCGGTACCCCACCTTAGAAAGTCCCTAAGG	pcDNA3.1/zeo/CST
pCST(1-36)EGFP	GCCTCGAGCCATGACTCTGCTGCCAAAGAAGCC GCGGATCCTGGAGGTACCACATAGGAGTAC	pcDNA3.1/zeo/CST
pCST(1-63)EGFP	GCCTCGAGCCATGACTCTGCTGCCAAAGAAGCC GCGAATTCGTGGCTGCCACTGGCTCATTGG	pcDNA3.1/zeo/CST
pCST(10-36)EGFP	CATGGCTCGAGATCTGAGTCC AAGTCCAAGGCCAAGGGGTTAC	pCST(1-36)EGFP

[a] The restriction sites introduced for sub-cloning are underlined, and the plasmid DNA used as the template for the PCR is shown.

Nut Mix F12 (1:1), fetal calf serum, penicillin, and streptomycin were from Invitrogen (Karlsruhe, Germany).

Plasmid Constructions. The generation of the pTRE-CST-HA plasmid has been described (*4*). A plasmid encoding CST with a C-terminal enhanced green fluorescent protein (CST-EGFP) was generated by PCR using the oligonucleotides shown in Table 1. The PCR product was subcloned into pEGFP-N3 (Clontech, CA) using *Xho*I and *Kpn*I. Deletion mutants CST(1-36)EGFP and CST(1-63)EGFP were generated by PCR using full-length murine CST cDNA as the template. The primer pairs used are listed in Table 1. For the construct, CST(10-36)EGFP primers were designed to allow amplification of the whole CST(1-36)EGFP and CST-EGFP plasmids, respectively, except for the deletion to be introduced (see Table 1). Oligonucleotides were phosphorylated using T4 polynucleotide kinase. PCR was done using Phusion DNA polymerase (Finnzymes/New England Biolabs, MA) according to instructions provided by the manufacturer. PCR conditions were 98 °C for 30 s followed by 25 cycles with 20 s/98 °C, 30 s/60 °C, and 120 s/72 °C. The PCR product was phenol/chloroform extracted, ligated, and the template plasmid removed by *Dpn*I digestion before transformation. All constructs were confirmed by DNA sequencing.

Generation of Rabbit Polyclonal CST Antiserum (ST2). The peptide KLSSRDKLAEFLQDPDRYYD (corresponding to amino acids 186−205 of murine CST) was coupled to keyhole limpet hemocyanin (KLH), and additional N-terminal cystein residues and the peptide-KLH conjugates were used to immunize White New Zealand rabbits (Lammers, Euskirchen, Germany) as described (*18*). For the immunization protocol, special permission according to the German Law on the Protection of Animals was obtained from the Bezirksregierung Köln.

Cell Culture and Transfections. Wild-type Chinese hamster ovary (CHO) cells (clone CHO-K1) were maintained in DMEM/Nut Mix F12 (1:1) supplemented with 5% fetal calf serum, 2 mM glutamine, 100 U/mL penicillin, and 100 μg/mL streptomycin. Baby hamster kidney (BHK) and green monkey kidney (COS-7) cells were grown in DMEM supplemented with 10% fetal calf serum, 2 mM glutamine, 100 U/mL penicillin, and 100 mg/mL streptomycin. Plasmid DNAs were purified by Qiagen plasmid purification columns following the instructions given by the manufacturer (Qiagen, Hilden, Germany). For transient transfections of BHK cells, 2×10^6 cells were seeded on 6-cm dishes and grown overnight. Cells were transfected with different plasmids using the Lipofectamine Plus protocol as provided by the manufacturer (Invitrogen, Karlsruhe, Germany). CHO and COS-7 cells were transfected using ExGen 500 (MBI Fermentas, St. Leon-Rot, Germany) following the instructions given by the manufacturer. For immunofluorescence staining, cells were seeded onto glass coverslips in 24-well plates (100,000 cells per well) and transfected with 1 μg of plasmid DNA and 3.3 μL of ExGen 500 in 500 μL of OptiMEM medium (Invitrogen, Karlsruhe, Germany). In some experiments, cells were treated with 10 μg/mL Brefeldin A (BFA; Sigma, Taufkirchen, Germany) for 100 min before fixation. Cycloheximide treatment was done using 500 μg/mL cycloheximide (Sigma) for 4 h.

Indirect Immunofluorescence. Cells on glass coverslips were fixed in 4% paraformaldehyde in PBS for 10 min. Cells were then washed three times with PBS and permeabilized with 0.3% Triton X-100 for 15 min. After incubation with 0.2% gelatine in PBS for 30 min, cells were incubated with primary antibodies in 0.2% gelatine in PBS for 1 h at room temperature. The following primary antibodies were used: mouse anti-HA monoclonal antibody 12CA5 (3 μg/mL), mouse anti-EGFP (1:500) rabbit anti-α-manosidase II antiserum (1:1,000), rabbit anti-rat mannose 6-phosphate receptor (MPR300; 1:500), and rabbit anti-mouse CST antiserum ST2 (1:500). After washing with PBS, cells were incubated with the relevant secondary antibodies: goat anti-sheep (Cy3 conjugated) (1:400), anti-mouse Cy2, and anti-rabbit Cy3, all from Jackson Immuno Research Laboratories (PA). Immunofluorescence was viewed using a Zeiss LSM 510 META confocal microscope. In some experiments, immunofluorescence was viewed using an Axiovert 100 M microscope (Carl Zeiss, Jena, Germany), and z-stacks were deconvoluted using the regularized inverse filter algorithm.

SDS−PAGE and Western Blotting. SDS−PAGE and Western blotting were done as described elsewhere (*19*). The following primary antibodies were used: rabbit anti-EGFP (1:5,000) and rabbit anti-CST (ST2; 1:2,000). Anti-mouse Ig-peroxidase conjugate and anti-rabbit Ig-peroxidase conjugate (Jackson Immuno Research Laboratories, PA) were used as secondary antibodies. Signal detection was performed after washing the membranes in PBS containing 0.05% Tween-20 with horseradish peroxidase-labeled secondary antibodies using ECL reagent (Amersham Biosciences, Freiburg, Germany).

Cell Surface Biotinylation. Transfected CHO cells were washed in ice-cold biotinylation buffer (10 mM sodium phosphate (pH 8.0), 10 mM KCl, and 135 mM NaCl) and

incubated in 1 mg/mL sulfo-NHS-SS-biotin (Pierce, Rockford) in biotinylation buffer for 3 h at 4 °C under constant shaking. After washing again with biotinylation buffer, cells were lysed in 50 mM imidazol (pH 7.0), 150 mM NaCl, and 0.5% Triton X-100. Biotinylated proteins were precipitated using streptavidin-agarose (Pierce). Precipitates were washed with 0.1% Triton X-100, 20 mM Tris-HCl (pH 7.4), and 150 mM NaCl. Unbound proteins were precipitated using chloroform/methanol. Samples were separated by SDS−PAGE and analyzed by Western blot.

Metabolic Labeling and Immunoprecipitation. Transfected cells were incubated in methionine-free DMEM medium (Invitrogen, Karlsruhe, Germany) for 1 h and then labeled with [^{35}S]-methionine (specific activity >39 TBq/mmol) (Amersham Biosciences, Freiburg, Germany) in the same medium containing 4% dialyzed fetal calf serum. The amount of radioactivity (80−150 μCi) as well as the time for pulse (5−180 min) and chase incubations varied in different experiments. Transfected BHK cells were lysed 48 h post-transfection by the addition of 0.5 mL/dish of lysis buffer A containing 20 mM Tris-HCl (pH 8), 150 mM NaCl, 1 mM EDTA (pH 8), and 1% Triton X-100. The protocols for metabolic labeling with [^{35}S]-methionine have been described in detail (*20*). Mouse CST, CST-HA, and CST-EGFP were immunoprecipitated with rabbit anti-CST antiserum (ST2) and mouse anti-HA Ig 12CA5 (Roche, Mannheim, Germany).

Endoglycosidase H Treatment. Transfected cells were radioactive-labeled with [^{35}S]-methionine as mentioned before. Cells were then resuspended in 100 μL of buffer A containing 20 mM Tris-HCl (pH 6), 150 mM NaCl, and 1% Triton X-100. The eluted samples were divided in half and incubated overnight at 37 °C with or without 50 mU/mL endoglycosidase H (Roche Molecular Biochemicals) in the presence of protease inhibitors.

After glycosidase digestion, samples were incubated overnight with mouse anti-HA Ig 12CA5 at 4 °C, and immunoprecipitates were recovered and separated by SDS−PAGE.

Glycerol Gradient Centrifugation. Transfected cells were lysed with buffer A (20 mM Tris-HCl at pH 8, 150 mM NaCl, 1 mM EDTA, and 1% Triton X-100) and centrifuged at 2,000*g* for 10 min at 4 °C. The post-nuclear supernatant was centrifuged at 100,000*g* for 30 min at 4 °C. Supernatants were laid on a 11 mL 5−35% (w/v) (in the case of CST-EGFP) or 1−27% (w/v) (in the case of CST(1-36)EGFP) linear glycerol gradient containing buffer A. Parallel gradients were laid with 0.6 mg of each of the following molecular mass markers (purchased from Amersham Biosciences, Freiburg, Germany): lysozyme (hen egg white; 14.3 kDa), ovalbumin (44 kDa), albumin (67 kDa), aldolase (150 kDa), and catalase (240 kDa) in buffer A. Gradients were centrifuged for 16 h at 35,000 rpm and 4 °C in an SW41 rotor (Beckman, Fullerton, CA) and fractionated in 0.5-mL aliquots from the top. Aliquots of each fraction (50 μL) were resolved by SDS−PAGE, and proteins were either stained with Coomassie Brilliant Blue (molecular mass markers) or detected by Western blotting (see above).

Fluorescence Correlation Spectroscopy (FCS). For fluorescence correlation spectroscopy, BHK cells were transiently transfected as described above. All proteins were produced as EGFP fusion proteins. FCS setup and instrumentation were described elsewhere (*21*). Briefly, measurements were performed 48 h post-transfection with a ConfoCor instrument (Zeiss, Jena, Germany). For excitation, the 488 nm line of an argon laser was focused through a water immersion objective (C-Apochromat, 63×, NA 1.2) into the Golgi membrane (laser power: p_{514nm} = 14.2 −109 kW/cm^2). Pinhole size was set to 40 μm. Emitted fluorescence was separated from the excitation light with a dichroic filter (FT 510) and a bandpass filter (EF 515-565). The fluctuations in intensity were detected by an avalanche single photon counting module. The signal was correlated online to data acquisition with a digital hardware correlator (ALV-5000, ALV, Langen, Germany). The illuminated volume element was positioned on the Golgi membrane both by visual inspection in the *x*-/*y*-direction and by motor aided scanning of the fluorescence of the cell in the *z*-direction.

RESULTS

CST Localizes to the Golgi Apparatus. In order to determine the subcellular localization of CST, we used HA- and enhanced green fluorescent protein (EGFP)-tagged CST variants, in which the HA peptide or EGFP protein were fused to the carboxyl-terminus of murine CST (CST-HA and CST-EGFP). CHO cells were transiently transfected with plasmids encoding CST-EGFP or CST-HA. Twenty to 24 h later, cells were treated with Brefeldin A (BFA) for 100 min, which induces a redistribution of Golgi enzymes into the ER, without affecting the TGN (*22*). Cells were fixed and processed for immunofluorescence using murine antibodies directed against the HA- (Figure 1A and B) or EGFP-tag (Figure 1C). Simultaneously, cells were stained with rabbit antisera directed against α-mannosidase II (Figure 1A) or the mannose 6-phosphate receptor (MPR300) (Figure 1B and C), which localizes to the TGN (*23*). Cells were examined by confocal microscopy. A partial co-localization of CST-HA with α-mannosidase II could be observed (Figure 1A), indicating the localization of CST in the Golgi apparatus. The partial co-localization with MPR300 (Figure 1B) suggested that CST-HA might also be present in the TGN. In order to further discriminate between trans-Golgi and TGN, cells were treated with BFA. The juxta-nuclear Golgi-like staining pattern of CST-HA as well as α-mannosidase II disappeared after BFA treatment, and CST-HA staining appeared as tubular structures (Figure 1A). The staining pattern of MPR300 did not change after BFA treatment, and there was no co-localization of CST-HA or CST-EGFP and MPR300 in BFA treated cells (Figure 1B and C). From these observations, we conclude that CST localizes to the Golgi apparatus in CHO cells but not to the TGN.

Transmembrane Domain of CST Contains a Golgi Localization Signal. In order to evaluate which part of CST determines Golgi localization, the 36 and 63 most N-terminal amino acid residues of CST were fused to EGFP, yielding the constructs CST(1-63)EGFP and CST(1-36)EGFP, respectively (Figure 2A and B). Intracellular localization of these fusion proteins was examined by immunofluorescence in transiently transfected CHO cells. Green fluorescence of both constructs partially co-localized with α-mannosidase II (Figure 2C), and the Golgi-like staining pattern was BFA-sensitive (data not shown), demonstrating that the 36 most N-terminal residues of CST contain sufficient information for Golgi localization. A Golgi staining pattern was also observed after deleting the cytosolic amino acids 2−9 of

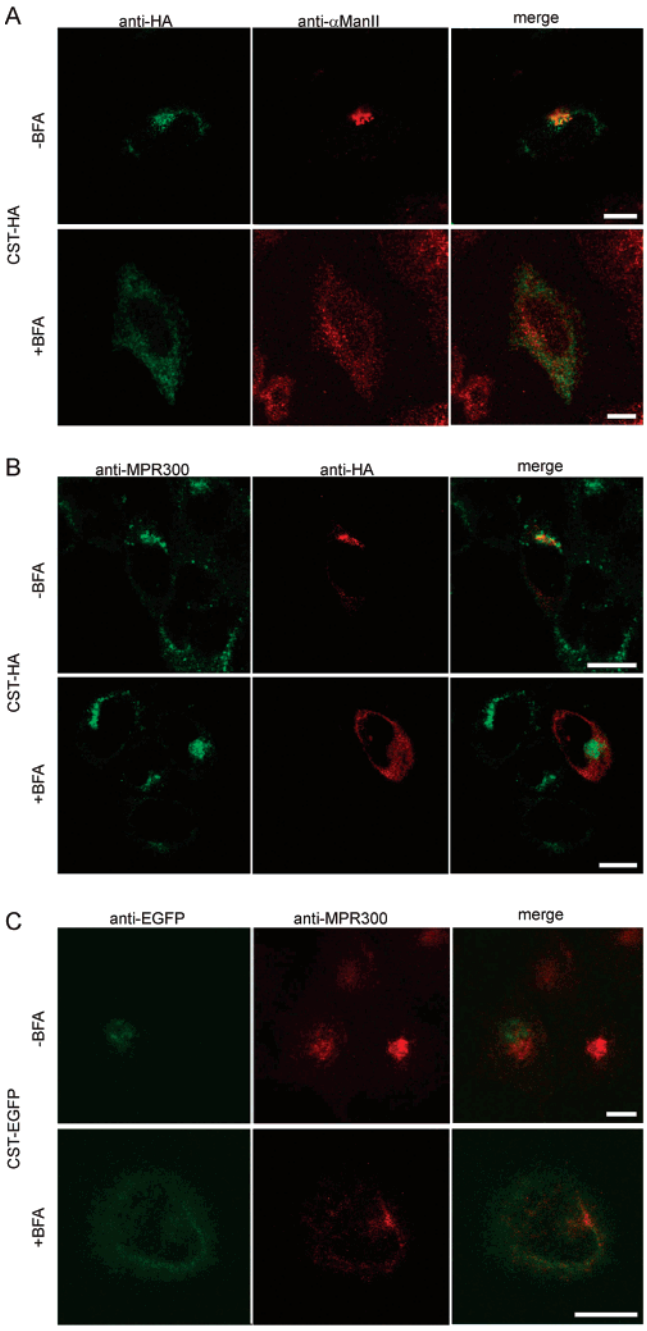

FIGURE 1: Golgi localization of murine CST. CHO cells were transiently transfected with plasmids encoding CST-HA (A and B) or CST-EGFP (C). Cells were treated for 100 min with 10 μg/mL Brefeldin A (+BFA) before fixation and stained with the indicated antibodies: (A) mouse anti-HA and rabbit anti-α mannosidase II (αManII; medial Golgi marker), (B) mouse anti-HA and rabbit anti-mannose 6-phosphate receptor (MPR300; TGN marker), and (C) mouse anti-EGFP and rabbit anti-MPR300. Immunofluorescence was viewed using a Zeiss LSM 510 META confocal microscope. The scale bars are 10 μm.

construct CST(1-36)EGFP, creating construct CST(10-36)-EGFP (Table 1), which contains only the transmembrane domain and the flanking basic residues (data not shown).

In order to examine whether the CST-EGFP fusion protein resides only transiently in the Golgi apparatus and exclude the possibility that CST-EGFP is predominantly sorted to the plasma membrane, we performed cell surface biotinylation experiments to detect any cell surface located fusion proteins. As shown in Figure 3A, only a minor fraction of

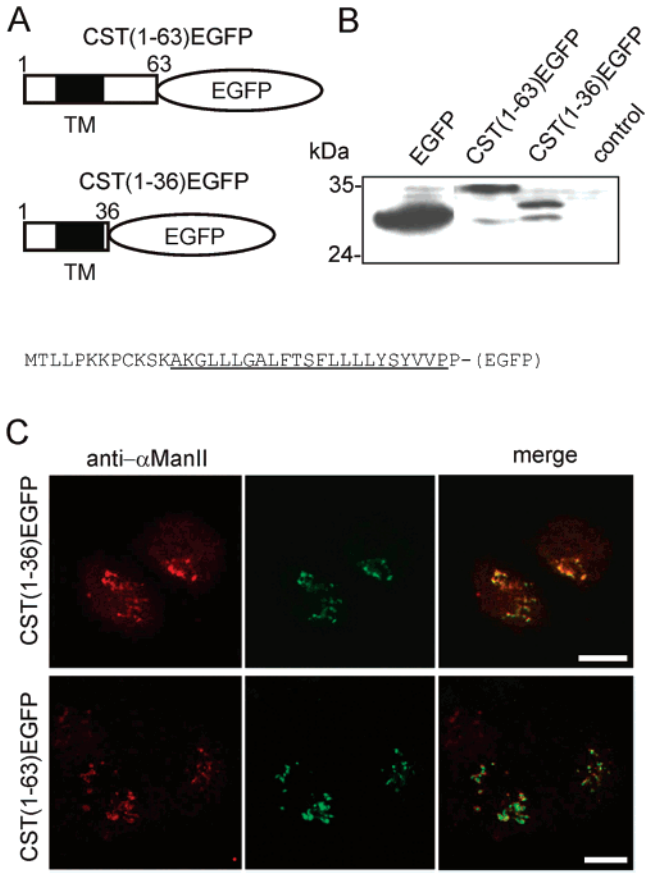

FIGURE 2: Transmembrane domain of CST determines Golgi localization. (A) Schematic representation of constructs CST(1-63)EGFP and CST(1-36)EGFP. TM, transmembrane region. The amino acid residues of the CST(1-36) mutant is shown. Underlined are the putative transmembrane regions as predicted by the TMHMM 2.0 program at http://www.cbs.dtu.dk. (B) Western blot analysis of cell lysates from CHO cells transiently transfected with the plasmids pEGFP-N3, CST(1-63)EGFP, CST(1-36)EGFP, or untransfected cells (control). Membranes were stained with anti-EGFP antiserum, and bound secondary antibodies were visualized by enhanced chemiluminescence detection. (C) CHO cells were transiently transfected with plasmids encoding CST(1-63)EGFP or CST(1-36)EGFP, fixed with 4% paraformaldehyde, permeabilized, and stained with rabbit anti-α mannosidase II (αManII). Immunfluorescence of the bound secondary antibody and the EGFP signal were viewed by confocal microscopy. The scale bars are 10 μm.

CST-EGFP localized to the cell surface. In accordance with the full-length protein, CST(1-36)EGFP also is mainly intracellularly localized (Figure 3A). These data confirmed stable Golgi localization of full-length CST as well as CST-(1-36)EGFP. To control for surface biotinylation efficiency, we performed Western blots with an antibody against PSA-NCAM, a cell adhesion molecule expressed by CHO cells. Only a minor fraction of PSA-NCAM was not biotinylated, confirming efficient cell surface biotinylation (Figure 3B). As a negative control, we biotinylated cells that were transiently transfected with a vector encoding β2-adrenergic receptor with a C-terminal EGFP (*24*). Because biotinylation can only take place at lysine residues and there is no lysine on the extracellular parts of the β2-adrenergic-receptor, biotinylation of β2-adrenergic-receptor-EGFP (β2-adr-EGFP) could not be detected (Figure 3B).

Characterization of CST Antiserum ST2. A polyclonal CST antiserum (ST2) was generated by the immunization of rabbits with a peptide encompassing amino acids 186−205

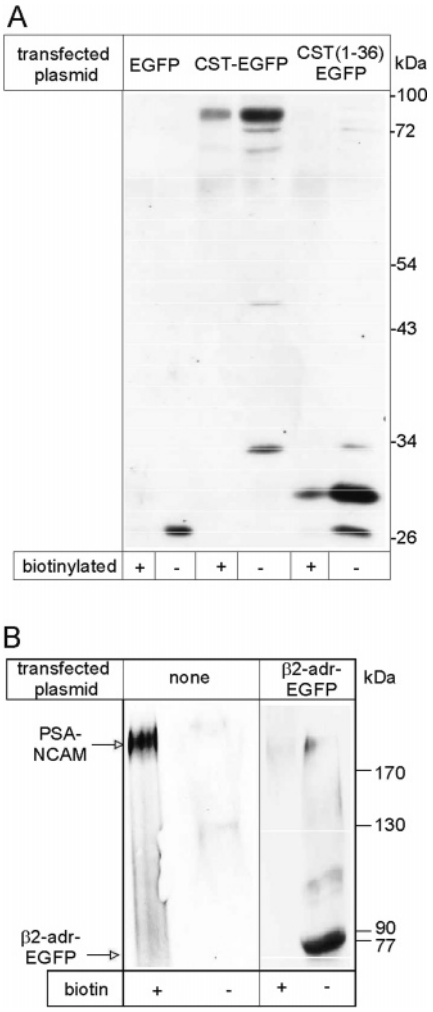

FIGURE 3: Biotinylation of cell surface proteins. (A) Cells were transiently transfected with the plasmids indicated on the top. Two days after transfection, cells were incubated in 1 mg/mL sulfo-NHS-SS-biotin (see Materials and Methods). After washing, cells were lysed, and the biotinylated proteins were isolated using streptavidin-agarose. Samples were separated by SDS−PAGE and analyzed by Western blot using rabbit anti-EGFP. Lanes containing streptavidin-purified biotinylated proteins are indicated by +, whereas the remaining non-biotinylated intracellular proteins that did not bind to streptavidin are indicated by −. (B) As a positive control for the biotinylation experiment, Western blots were stained with an antibody against PSA-NCAM in untransfected CHO cells (none). Only a minor fraction of PSA-NCAM was not biotinylated. As a negative control, CHO cells were transfected with a plasmid expressing β2-adrenergic-receptor-EGFP, which has no lysine residues on its extracellular parts.

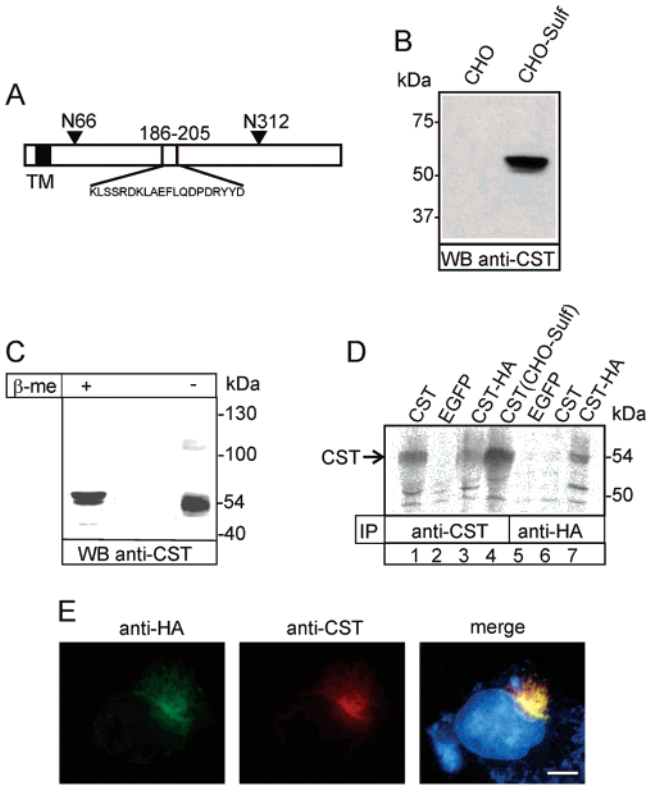

FIGURE 4: Characterization of rabbit CST antiserum. (A) Schematic representation of CST protein, indicating the position of the peptide used for the immunization of rabbits (186−205). Triangles indicate *N*-glycosylation sites at amino acid residues 66 and 312; TM, transmembrane domain. (B) Total cell lysates (50 μg of protein per lane) of CHO and CHO-Sulf cells (expressing murine CST) were resolved by SDS−PAGE and analyzed by Western blotting (WB) using the CST antiserum ST2. (C) CHO cells stably transfected with CST (CHO-Sulf) were lysed in 1% Triton X-100, and 50 μg of protein were separated in 10% SDS−PAGE in the presence (+β-me) or absence (−β-me) of β-mercaptoethanol. Western blot analysis was performed with anti-CST antiserum. (D) BHK cells transiently transfected with plasmids encoding CST, EGFP, CST-HA cDNAs, and CHO cells stably transfected with CST (CHO-Sulf) were lysed in buffer A containing 1% Triton X-100 (Materials and Methods) and immunoprecipitated (IP) with CST antiserum or anti-HA antibody, respectively. A 54 kDa protein was immunoprecipitated in cells expressing CST (lanes 1, 3, and 4) but not in control cells (lane 2). The CST-HA fusion protein was also immunoprecipitated with the anti-HA antibody from transiently transfected cells (lane 7). In contrast, cells that were transfected with untagged CST could not be precipitated with anti-HA antibody (lane 6). (E) COS cells were transiently transfected with CST-HA expression plasmid and simultaneously stained with anti-HA antibody and rabbit CST-antiserum (ST-2). Co-localization of both antibodies confirmed the specificity of the ST-2 antiserum. Nuclei were stained with DAPI. The scale bar is 10 μm.

of the murine CST (Figure 4A). ST2 detected a single polypeptide of 54 kDa in Western blots of lysates from CHO cells stably transfected with murine CST cDNA (CHO-Sulf) (*4*) but not in non-transfected CHO cells (Figure 4B). In Western blots of CHO-Sulf cells under non-reducing conditions, an additional protein with an apparent molecular mass of 110 kDa was detected, suggesting that a minor fraction (<10%) of CST forms disulfide-dependent homodimers (Figure 4C). Identical results were obtained when cell lysis was carried out in the presence of 100 mM iodoacetamide (data not shown). However, it remains to be determined whether these SDS-resistant dimers are formed by intermolecular disulfide bonds or dependent on intramolecular disulfide bonds.

To examine whether the CST antiserum (ST2) is able to immunoprecipitate CST protein, cells transiently expressing CST or CST-HA were metabolically labeled with [^{35}S]-methionine and lysed, and CST was precipitated from the cell lysates with CST antiserum or anti-HA antibody, respectively (Figure 4D). In addition, COS cells were transiently transfected with the CST-HA construct and processed for immunofluorescence using CST antiserum and the anti-HA antibodies. This revealed complete co-localization of anti-HA and CST antiserum immunoreactivity, further demonstrating the specificity of the antiserum (Figure 4E).

Oligomerization of CST. In order to examine the quaternary structure of CST, co-immunoprecipitations and glycerol

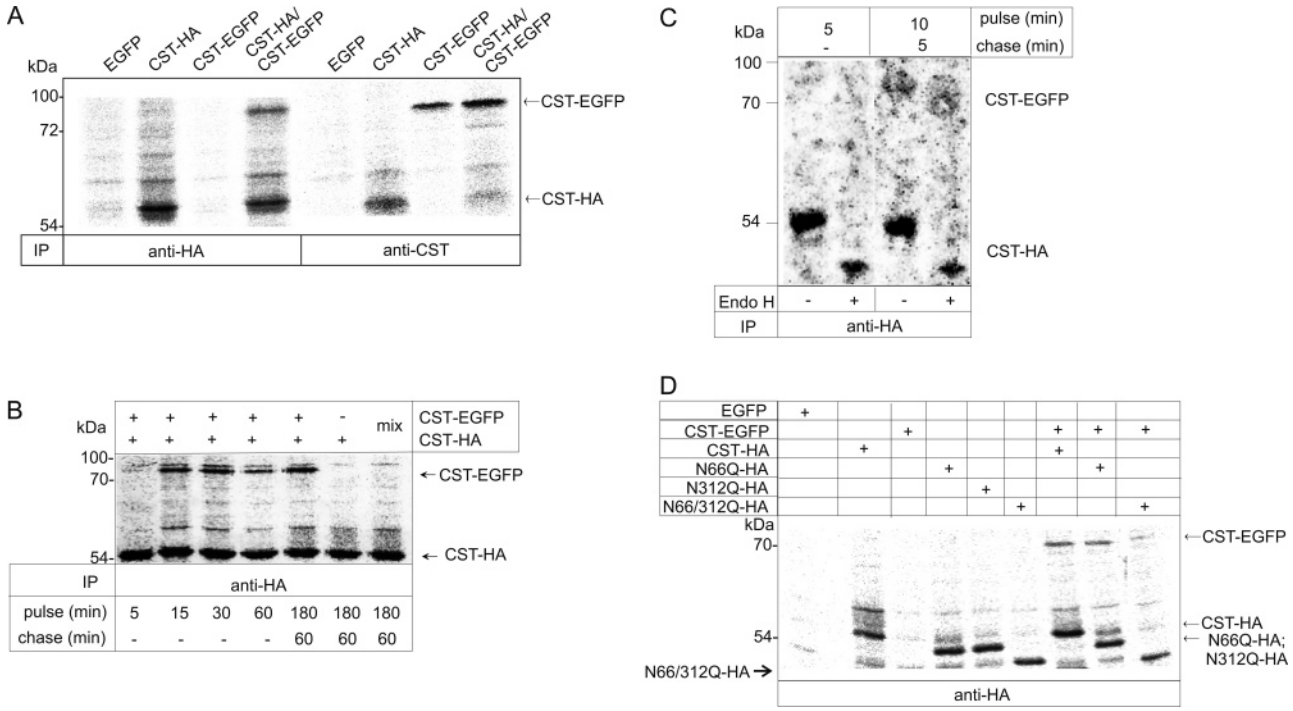

FIGURE 5: Immunoprecipitation of CST oligomers. (A) BHK cells were transiently transfected with expression plasmids containing the mouse CST-EGFP or CST-HA cDNAs as indicated on the top. As a negative control, cells were transfected with a plasmid containing EGFP cDNA. CST-HA/CST-EGFP indicates co-transfection of both constructs. Two days after transfection, cells were labeled metabolically with 100 μCi of [^{35}S]-methionine for 2 h and chased for 2 h. CST was immunoprecipitated from cell lysates initially with anti-HA antibody (left part), and in the next step, supernants of the same samples were precipitated with anti-CST antibody (right part). Immunoprecipitates were resolved by SDS−PAGE, and radioactivity was visualized with a Fuji Bioimager. (B) Time dependence of CST oligomerization. BHK cells were transiently transfected with expression plasmid containing CST-HA cDNA or co-transfected with CST-EGFP plasmid (CST-HA/CST-EGFP) as indicated on the top. Transfected cells were pulse labeled for 5 to 180 min with 150 μCi of [^{35}S]-methionine and chased for different times as indicated. Oligomerization of CST could be clearly observed after precipitation with anti-HA antibody after 15 min of pulse labeling. However, after 5 min a faint co-immunoprecipitated CST-EGFP could be detected. As a control for oligomerization, BHK cells were transfected separately with CST-HA and CST-EGFP plasmids. Cells were separately lysed and mixed (mix) prior to immunoprecipitation with the anti-HA antibody. No oligomerization of CST-HA and CST-EGFP could be observed in this case. (C) BHK-cells were co-transfected with CST-HA and CST-EGPF plasmids. Cells were pulse labeled with [^{35}S]-methionine for 5 or 10 min, then lysed and divided in half. The samples were incubated in the absence (lanes 1 and 3) or presence (lanes 2 and 4) of endoglycosidase H (Endo H) and immunoprecipitated with anti HA-antibody. CST-HA and CST-EGFP were Endo H sensitive. (D) BHK cells were transiently transfected with expression plasmids encompassing wild-type HA- or EGFP-epitope tagged CST (CST-HA; CST-EGFP) or CST-HA glycosylation mutants in which the relevant asparagine residues were changed to glutamine, individually (N66Q; N312Q) or in combination (N66/312Q). Two days after transfection, cells were metabolically labeled with 100 μCi of [^{35}S]-methionine for 1 h and chased for 1 h. Wild-type mouse CST and CST mutants were immunoprecipitated with anti-HA antibody. Oligomerization of CST could be observed with all N-glycosylation mutants. Cells transfected with EGFP plasmid served as the negative control.

density gradient centrifugations as well as fluorescence correlation spectroscopy (FCS) of living cells were performed. To investigate the oligomerization status of CST, BHK cells were co-transfected with plasmids encoding CST-HA or CST-EGFP cDNA and metabolically labeled with [^{35}S]-methionine. Cells were lysed in buffers containing 1% Triton X-100 followed by immunoprecipitation with anti-HA antibody 12CA5 or anti-CST antiserum ST2 (Figure 5).

The left part of Figure 5A shows samples that were immunoprecipitated initially with anti-HA antibody. In the next step, supernants of the same samples were incubated with anti-CST antiserum ST2, as indicated on the right. Fusion proteins of 54 kDa (CST-HA) or 81 kDa (CST-EGFP), as expected from the calculated molecular masses of these proteins, were precipitated.

When BHK cells were co-transfected with CST-HA and CST-EGFP expression plasmids, both proteins of 54 and 81 kDa were detected in the anti-HA immunoprecipitates (Figure 5A, CST-HA/CST-EGFP). Because the CST-EGFP fusion protein does not contain a HA-tag, the presence of this protein in the HA-immunoprecipitates can only be explained by oligomerization of CST-HA and CST-EGFP polypeptides.

To elucidate whether oligomerization occurs before or after CST leaves the ER, BHK cells were transiently transfected with CST-HA- and CST-EGFP-expressing plasmids, respectively, and pulse-labeled with [^{35}S]-methionine for 5 to 180 min. As shown in Figure 5B, CST-EGFP fusion protein was clearly co-immunoprecipitated with the HA-antibody after 15 min of pulse labeling. However, after 5 min a faint co-immunoprecipitated CST-EGFP fusion protein could be detected. As a control, cells were separately transfected with CST-HA and CST-EGFP fusion proteins, and lysates were combined before immunoprecipitation (Figure 5B, mix). Under these conditions, CST-EGFP was not co-immunoprecipitated with CST-HA, demonstrating that oligomers did not form after cell lysis.

In addition, endoglycosidase H (Endo H) was used to digest high-mannose-type oligosaccharides of anti-HA immunoprecipitates of CST-HA and CST-EGFP co-expressing BHK cells. Figure 5C shows the Endo H digestion of pulse-labeled proteins. The samples were immunoprecipitated after Endo H treatment with anti-HA antibody. When cells were

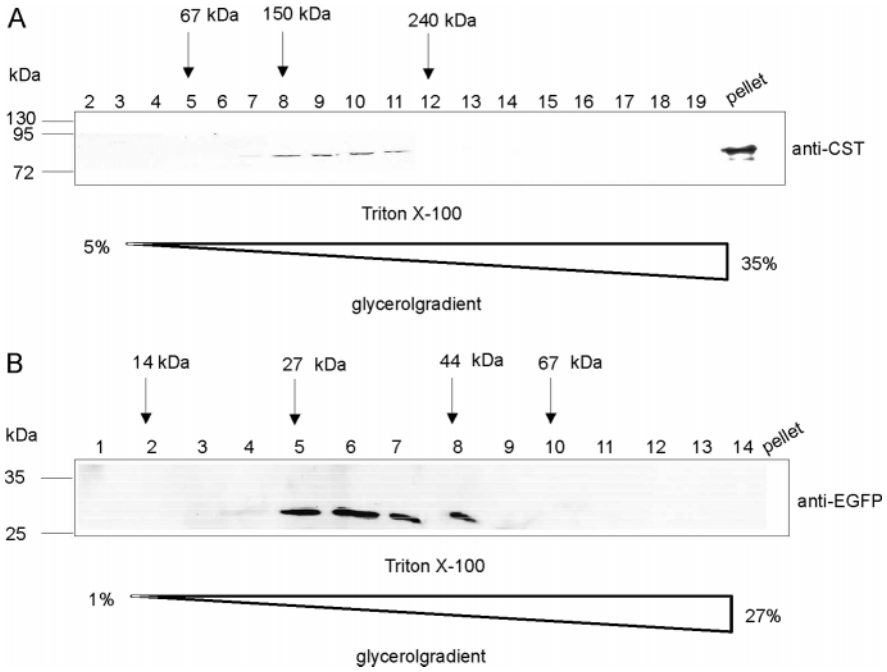

FIGURE 6: Glycerol gradient centrifugation of CST-dimers. Transiently transfected BHK cells expressing mouse CST-EGFP (used in A) or CST(1-36)EGFP (used in B) were lysed in buffers containing 1% Triton X-100 as indicated. The post-nuclear fraction was centrifuged at 100,000*g* for 30 min. Supernatants were applied to a 5−35% (A) or 1−27% (B) glycerol gradient subjected to centrifugation as described in the Materials and Methods section. Glycerol gradient fractions and the 100,000*g* pellets were examined by 10% SDS−PAGE and Western blot analysis with anti-CST antiserum (A) or anti-EGFP antiserum (B). The arrows show positions of molecular mass markers: lysozyme (hen egg white; 14 kDa), ovalbumin (44 kDa), albumin (67 kDa), aldolase (150 kDa), and catalase (240 kDa).

pulse labeled for 10 min and chased for 5 min, CST-HA and CST-EGFP were sensitive to endoglycosidase H, strongly suggesting that oligomerization of CST occurs in the ER.

We recently showed that N-glycosylation of CST is necessary to form a fully active enzyme (*4*). Two N-glycosylation sites at N66 and N312 are present and used in murine CST (Figure 4A). To determine whether the removal of N-glycosylation sites affects dimerization of the enzyme, CST-HA mutants lacking single (N66Q-HA) or both (N66/312Q-HA) N-glycosylation sites, respectively, were transiently transfected separately or co-transfected with wild-type CST-EGFP and immunoprecipitated from cell lysates using anti-HA antibody. Because the CST-EGFP fusion protein is not HA tagged, its presence in the immunoprecipitation is indicative of oligomerization. Figure 5D shows that the removal of *N*-glycans did not interfere with the ability to co-immunoprecipitate the CST-EGFP fusion protein. Moreover, preliminary experiments with CST protein, in which the transmembrane region was deleted, also showed dimerization after immunoprecipitation with the wild-type CST, when both constructs were co-transfected in BHK or COS-7 cells (unpublished data).

CST Is a Homodimer. To determine the degree of CST oligomerization, cells transiently expressing CST-EGFP (81 kDa) were homogenized in lysis buffer containing 1% Triton X-100, and afterward, a 100,000*g* supernatant was subjected to centrifugation through a glycerol density gradient in the same lysis buffer. After centrifugation, fractions were collected and analyzed by Western blot with anti-CST (ST2) antiserum as indicated in Figure 6. In the presence of 1% Triton X-100, CST-EGFP was found in fractions 8−11. According to the size of proteins used as standards (aldolase 150 kDa and catalase 240 kDa), the localization of the 81 kDa CST-EGFP fusion protein suggests dimerization of CST-EGFP. No monomers of CST-EGFP were detected (Figure 6A). Analysis of the 100,000*g* pellet, however, showed that part of the CST-EGFP protein was insoluble in Triton X-100, which might be due to the formation of large aggregates (Figure 6A; pellet). Whereas in the presence of the strong ionic detergent, *N*-laurylsarcosine CST-EGFP was solubilized completely (data not shown). The same result was obtained with the native, untagged CST protein (data not shown). The glycerol gradient experiment was also done with construct CST(1-36)EGFP in the presence of 1% Triton X-100. Figure 6B shows that in contrast to CST-EGFP, CST(1-36)EGFP migrated exclusively as a monomer. The same result was obtained with CST(1-63)EGFP (data not shown). These results show that CST-EGFP forms homodimers and that dimerization is mediated by the CST lumenal domain.

Fluorescence Correlation Spectroscopy of CST in Living Cells. To prove that dimerization of CST also occurs in living cells, we used fluorescence correlation spectroscopy (FCS). FCS allows one to measure the mobility of fluorescent molecules in defined small volumes within a cell. The autocorrelation function of the temporal fluctuations of the fluorescence signal measured in the small volume allows one to calculate the diffusion times and subsequently the molecular mass of the fluorescent particles. Soluble EGFP was found to diffuse in the cytosol of these cells with a diffusion time constant τ_D of 0.45 ± 0.12 ms ($n = 35$) and a count rate (brightness) of 2.05 ± 0.2 counts per molecule, corresponding to a calculated diffusion coefficient $D = 2.19 \times 10^{-7}$ cm^2/s in agreement with previous reports (*25*).

The lateral mobilities of CST-EGFP and CST(1-36)EGFP fusion proteins and EGFP were investigated in BHK cells (Figure 7; Table 2). The intracellular fluorescence profile obtained by moving an illuminated volume element of a sharply focused laser beam in the *z*-direction through the

Table 2: Comparison of Diffusion Coefficients

molecule	diffusion coefficient cm^2/s	abundance
CST-EGFP ($n = 55$)	$D_1 = 7.97 \pm 0.48 \times 10^{-8}$ $D_2 = 2.29 \pm 0.7 \times 10^{-9}$	$70 \pm 8\%$ $30 \pm 8\%$
CST(1−36)EGFP ($n = 11$)	$D_1 = 1.45 \pm 0.17 \times 10^{-7}$ $D_2 = 2.51 \pm 0.95 \times 10^{-9}$	$91 \pm 3\%$ $9 \pm 3\%$
EGFP ($n = 35$)	$D = 2.19 \pm 0.5 \times 10^{-7}$	100%

cell clearly indicated the position of the Golgi membranes in cells transfected with CST-EGFP as well as CST(1-36)-EGFP. The volume element was placed on the peak intensity indicating the presence of Golgi membranes, and the lateral mobilities of the fusion proteins were determined. The autocorrelation curve of the CST-EGFP fusion protein was clearly shifted toward higher diffusion times when compared with that of the truncated CST(1-36)EGFP construct (Figure 7), which migrated exclusively as a monomer (Figure 6B). For CST-EGFP, a quantitative evaluation of the autocorrelation curves revealed a dominating average diffusion time constant $\tau_{D1} = 1.25 \pm 0.08$ ms ($n = 55$) (accounting for $70 \pm 8\%$ of all CST-EGFP fusion proteins) and an even slower minor fraction of molecules with $\tau_{D2} = 43.64 \pm 19.09$ ms ($n = 55$) ($30 \pm 8\%$). Compared to that of EGFP, an increased count rate of 2.87 ± 0.45 counts per molecule was calculated for CST-EGFP, excluding the possibility that this protein forms higher oligomers as a dimer. By contrast, different diffusion time constants were measured for CST(1-36)EGFP with a major average diffusion time constant $\tau_{D1} = 0.69 \pm 0.09$ ms ($n = 11$) accounting for $91 \pm 3\%$ of the molecules and a small fraction of molecules displaying a slow diffusion time constant $\tau_{D2} = 39.90 \pm 24.30$ ms ($n = 11$) of $9 \pm 3\%$ (Figure 7).

Figure 7 shows the autocorrelation function ($G[\tau]$) as a function of variable τ, the time interval between different fluorescence intensity values. A brightness of 1.97 ± 0.56 counts per molecule was found for CST(1-36)EGFP. This value was not significantly different from the brightness of EGFP alone (see above), indicating that CST(1-36)EGFP exclusively forms monomers. Table 2 shows the comparison of diffusion coefficients of EGFP, CST-EGFP, and CST(1-36)EGFP.

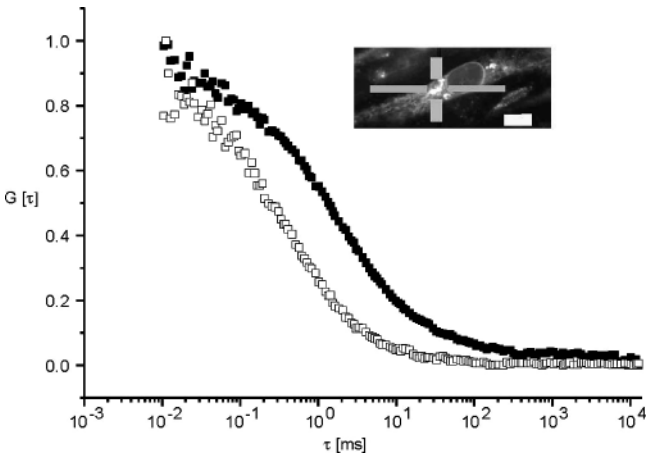

FIGURE 7: Detection of CST dimers using fluorescence correlation spectroscopy (FCS). Representative normalized autocorrelation curves are shown. (■) indicates autocorrelation of CST-EGFP in Golgi membranes of BHK cells with a diffusion time constant of $\tau_{D1} = 1.25 \pm 0.08$ ms ($n = 55$) and $\tau_{D2} = 43.64 \pm 19.09$ ms ($n = 55$); (□) shows autocorrelation of CST(1-36)EGFP bound to the Golgi membrane of BHK cells with $\tau_{D1} = 0.69 \pm 0.09$ ms ($n = 11$) and $\tau_{D2} = 39.90 \pm 24.30$ ms ($n = 11$). $G[\tau]$ indicates the autocorrelation function as a function of variable τ. (Inset) Position of the illuminated volume element on the Golgi membrane of BHK cells expressing CST-EGFP. The scale bar is 5 μm.

DISCUSSION

Our data provide strong evidence that murine CST localizes to the Golgi apparatus but not to the TGN. Farrer et al. (*17*) suggested that on the basis of the effect of BFA on sulfatide synthesis, CST is localized in the TGN. In the presence of BFA, sulfatide but not galactosylceramide synthesis was strongly reduced, suggesting uncoupling of the two reactions by the BFA block (*17*). Our data, which are based on direct immunodetection of the enzyme rather than its enzymatic activity, however, show that CST localization is affected by BFA. Moreover, an examination of deletion mutants of CST-EGFP fusion proteins showed that amino acid residues 10−36 that include the transmembrane domain contain sufficient information for stable Golgi localization and that additional parts of the stem region, other parts of the lumenal domain, or the amino-terminal cytosolic tail are not required.

Co-immunoprecipitation experiments demonstrated that CST is present as an oligomer. To determine the stochiometry of this oligomer, glycerol gradient centrifugation experiments were performed. We used CST-EGFP fusion proteins in these experiments, and the results suggest that these fusion proteins form dimers. When the CST lumenal domain was removed, the resulting construct CST(1-36)EGFP appeared exclusively as a monomer. This shows that the dimerization of CST-EGFP depends on the CST lumenal domain. Western blot analysis of stably transfected CHO cells under non-reducing conditions showed that only a minor fraction of CST formed disulfide bond-dependent dimers. Because almost all CST migrated as dimers in glycerol gradients, it can be concluded that most CST dimers are noncovalently bound. Interestingly, our data show that the oligomerization of CST is not dependent on N-glycosylation sites or the transmembrane domain of the protein.

Fluorescence correlation spectroscopy (FCS) is a proper method to obtain evidence for protein behavior by assessing the diffusion properties of the protein. Autocorrelation analysis and molecule brightness analysis (count rate) are complementary techniques. The autocorrelation function depends on the diffusion behavior and therefore mass and shape of the fluorescent particle. The count rate (brightness) is a measure of the number of fluorescent molecules within each moving particle.

FCS of CST-EGFP revealed that this molecule was mobile in Golgi membranes. For the major component accounting for about 70% of the molecules, a diffusion coefficient of $D_1 = 7.97 \times 10^{-8}$ cm^2/s was calculated. This value was in the range measured previously for the lateral mobilities of the β_2-adrenergic receptor and the $GABA_A$ receptor in the plasma membrane (*21*, *26*). In accordance with its monomeric status, the truncated CST(1-36)EGFP construct diffused considerably faster in Golgi membranes with $D_1 = 1.45 \times 10^{-7}$ cm^2/s than CST-EGFP. This 1.8-fold difference of the diffusion coefficients suggests a 6-fold mass difference, which is considerably larger than the mass difference

between the two proteins (81 kDa for CST-EGFP vs 31 kDa for CST(1-36)EGFP). The measured diffusion coefficients are consistent with our observation that CST-EGFP forms dimers. The difference of the diffusion coefficients between CST(1-36)EGFP and CST-EGFP is in good agreement with the calculated difference in molecular mass assuming monomeric CST(1-36)EGFP and dimeric CST-EGFP. Moreover, the brightness of the diffusing dimers of CST-EGFP was significantly higher than the brightness of CST(1-36)EGFP and EGFP monomers. Thus, CST-EGFP forms dimers *in vivo*.

The fact that the average brightness over all diffusing species was increased by only 50% may be explained by fluorescence quenching due to the presence of a larger protein domain fused to the EGFP domain. A significant fraction of 30% of the CST-EGFP molecules diffused even slower with $D_2 = 2.29 \times 10^{-9}$ cm^2/s. These molecules may represent CST-EGFP, which underwent interactions with other membrane proteins, the cytoskeleton, or membrane microdomains. Because the brightness for both diffusion time constants in the case of CST-EGFP is the same, our data strongly support the view that CST exists exclusively as a homodimeric protein in the Golgi apparatus of living cells and does not form higher homo-oligomers. Probably part of the Triton X-100 insoluble CST corresponds to the slower diffusing fraction of CST molecules.

In summary, our biochemical and biophysical approaches suggest that CST forms dimers, and we identified that the transmembrane region of CST is sufficient for stable Golgi targeting of a monomeric EGFP reporter protein. Dimerization of several proteins appear to be necessary for exit from the ER (*27*). Whether dimerization of CST is required for ER export remains to be determined because it is not possible to ascertain whether the CST(1-36)EGFP protein completely mimics the trafficking of the native CST protein. Similarly, hetero-oligomerization, which might be mediated by specific residues in the lumenal domain (*28*), has been suggested to be responsible for Golgi retention of glycosyltransferases (*16*). In addition, we were able to show that monomeric CST-(1-36)EGFP and CST(1-63)EGFP proteins were exclusively localized to the Golgi apparatus.

ACKNOWLEDGMENT

We thank Ivonne Becker for expert technical assistance.

REFERENCES

1. Tennekoon, G., Zaruba, M., and Wolinsky, J. (1983) Topography of cerebroside sulfotransferase in Golgi-enriched vesicles from rat brain, *J. Cell Biol. 97*, 1107−1112.
2. Honke, K., Tsuda, M., Hirahara, Y., Ishii, A., Makita, A., and Wada, Y. (1997) Molecular cloning and expression of cDNA encoding human 3′-phosphoadenylylsulfate:galactosylceramide 3′-sulfotransferase, *J. Biol. Chem. 272*, 4864−4868.
3. Hirahara, Y., Tsuda, M., Wada, Y., and Honke, K. (2000) cDNA cloning, genomic cloning, and tissue-specific regulation of mouse cerebroside sulfotransferase, *Eur. J. Biochem. 267*, 1909−1917.
4. Eckhardt, M., Fewou, S. N., Ackermann, I., and Gieselmann, V. (2002) N-glycosylation is required for full enzymic activity of the murine galactosylceramide sulphotransferase, *Biochem. J. 368*, 317−324.
5. Honke, K., Zhang, Y., Cheng, X., Kotani, N., and Taniguchi, N. (2004) Biological roles of sulfoglycolipids and pathophysiology of their deficiency, *Glycoconjugate J. 21*, 59−62.
6. Ogawa, D., Shikata, K., Honke, K., Sato, S., Matsuda, M., Nagase, R., Tone, A., Okada, S., Usui, H., Wada, J., Miyasaka, M., Kawashima, H., Suzuki, Y., Taniguchi, N., Hirahara, Y., Tadano-Aritomi, K., Ishizuka, I., Tedder, T. F., and Makino, H. (2004) Cerebroside sulfotransferase deficiency ameliorates L-selectin-dependent monocyte infiltration in the kidney after ureteral obstruction, *J. Biol. Chem. 279*, 2085−2090.
7. Zhang, Y., Hayashi, Y., Cheng, X., Watanabe, T., Wang, X., Taniguchi, N., and Honke, K. (2005) Testis-specific sulfoglycolipid, seminolipid, is essential for germ cell function in spermatogenesis, *Glycobiology 15*, 649−654.
8. Hirahara, Y., Bansal, R., Honke, K., Ikenaka, K., and Wada, Y. (2004) Sulfatide is a negative regulator of oligodendrocyte differentiation: development in sulfatide-null mice, *Glia 45*, 269−277.
9. Scherer, S. S. (1996) Molecular specialization at nodes and paranodes in peripheral nerve, *Microsc. Res. Tech. 34*, 452−461.
10. Honke, K., Hirahara, Y., Dupree, J., Suzuki, K., Popko, B., Fukushima, K., Fukushima, J., Nagasawa, T., Yoshida, N., Wada, Y., and Taniguchi, N. (2002) Paranodal junction formation and spermatogenesis require sulfoglycolipids, *Proc. Natl. Acad. Sci. U.S.A. 99*, 4227−4232.
11. Von Figura, K., Gieselmann, V., and Jaeken, J. (2001) in *The Metabolic and Molecular Basis of Inherited Disease* (Scriver, C. R., Beaudet, A. L., Valle, D., and Sly, W. S., Eds) pp 3695−3724, McGraw Hill, New York.
12. Jeyakumar, M., Butters, T. D., Cortina-Borja, M., Hunnam, V., Proia, R. L., Perry, V. H., Dwek, R. A., and Platt, F. M. (1999) Delayed symptom onset and increased life expectancy in Sandhoff disease mice treated with N-butyldeoxynojirimycin, *Proc. Natl. Acad. Sci. U.S.A. 96*, 6388−6393.
13. Dwek, R. A., Butters, T. D., Platt, F. M., and Zitzmann, N. (2002) Targeting glycosylation as a therapeutic approach, *Nat. Rev. Drug Discovery 1*, 65−75.
14. Marks, D. L., Wu, K., Paul, P., Kamisaka, Y., Watanabe, R., and Pagano, R. E. (1999) Oligomerization and topology of the Golgi membrane protein glucosylceramide synthase, *J. Biol. Chem. 274*, 451−456.
15. Sasai, K., Ikeda, Y., Tsuda, T., Ihara, H., Korekane, H., Shiota, K., and Taniguchi, N. (2001) The critical role of the stem region as a functional domain responsible for the oligomerization and Golgi localization of N-acetylglucosaminyltransferase V. The involvement of a domain homophilic interaction, *J. Biol. Chem. 276*, 759−765.
16. Colley, K. J. (1997) Golgi localization of glycosyltransferases: more questions than answers, *Glycobiology 7*, 1−13.
17. Farrer, R. G., Warden, M. P., and Quarles, R. H. (1995) Effects of brefeldin A on galactosphingolipid synthesis in an immortalized Schwann cell line: evidence for different intracellular locations of galactosylceramide sulfotransferase and ceramide galactosyltransferase activities, *J. Neurochem. 65*, 1865−1873.
18. Franken, S., Junghans, U., Rosslenbroich, V., Viebahn, C., and Kappler, J. (2003) Collapsin response mediator proteins of neonatal rat brain interact with chondroitin sulfate, *J. Biol. Chem. 278*, 3241−3250.
19. Yaghootfam, A., Gieselmann, V., and Eckhardt, M. (2005) Delay of myelin formation in arylsulfatase A deficient mice, *Eur. J. Neurosci. 21*, 711−720.
20. Yaghootfam, A., and Gieselmann, V. (2003) Specific hammerhead ribozymes reduce synthesis of cation-independent mannose 6-phosphate receptor mRNA and protein, *Gene Ther. 10*, 1567−1574.
21. Hegener, O., Prenner, L., Runkel, F., Baader, S. L., Kappler, J., and Häberlein, H. (2004) Dynamics of beta2-adrenergic receptor-ligand complexes of living cells, *Biochemistry 43*, 6190−6199.
22. Chege, N. W., and Pfeffer, S. R. (1990) Compartmentation of the Golgi complex: brefeldin-A distinguishes trans-Golgi cisternae from trans-Golgi network, *J. Cell Biol. 111*, 893−899.
23. Lin, S. X., Mallet, W. G., Huang, A. Y., and Maxfield, F. R. (2003) Endocytosed cation-independent mannose 6-phosphate receptor traffics via the endocytic recycling compartment en route to the trans-Golgi network and a subpopulation of late endosomes, *Mol. Biol. Cell 15*, 721−733.
24. Krasel, C., Bunemann, M., Lorenz, K., and Lohse, M. J. (2005) Beta-arrestin binding to the beta2-adrenergic receptor requires both receptor phosphorylation and receptor activation, *J. Biol. Chem. 280*, 9528−9535.
25. Chen, Y., Muller, J. D., Ruan, Q., and Gratton, E. (2002) Molecular brightness characterization of EGFP in vivo by fluorescence fluctuation spectroscopy, *Biophys. J. 82*, 133−144.

26. Meissner, O., and Häberlein, H. (2003) Lateral mobility and specific binding to GABA(A) receptors on hippocampal neurons monitored by fluorescence correlation spectroscopy, *Biochemistry 42*, 1667−1672.
27. Tu, L., Sun, T. T., and Kreibich, G. (2002) Specific heterodimer formation is a prerequisite for uroplakins to exit from the endoplasmatic reticulum, *Mol. Biol. Cell 13*, 4221−4230.
28. Sevier, C. S., and Machamer, C. E. (1998) Fragmentation of a Golgi-localized chimeric protein allows detergent solubilization and reveals an alternate conformation of the cytoplasmic domain, *Biochemistry 37*, 185−192.

BI700014Q